Supporting Information

Initial steps in forming the electrode electrolyte interface: H_2O adsorption and complex formation on the Ag(111) surface from combining Quantum Mechanics calculations and Ambient Pressure X-ray Photoelectron Spectroscopy

Jin Qian[#12], Yifan Ye[#345], Hao Yang[2], Junko Yano[3]*, Ethan J. Crumlin[4]*, William A. Goddard III[12]*

[1]Joint Center for Artificial Photosynthesis, California Institute of Technology, Pasadena, CA 91125, United States;

[2]Materials and Process Simulation Center, California Institute of Technology, Pasadena, CA 91125, United States;

[3]Joint Center for Artificial Photosynthesis, Lawrence Berkeley National Laboratory,

Berkeley, CA 94720, United States;

[4]Advanced Light Source, Lawrence Berkeley National Laboratory, Berkeley, CA 94720, United States;

[5]Chemical Sciences Division, Lawrence Berkeley National Laboratory, Berkeley, CA 94720, United States;

# These authors contributed equally

Email: jyano@lbl.gov; ejcrumlin@lbl.gov; wag@caltech.edu

Supplementary Information Contents

Carbon Contamination Discussion:

Unavoidably, there's possibility of contamination of CO_xH_y species during the H_2O dosing process. There is quite a lot debates regarding to the origination of this contaminations[1]. As shown in Fig. S1, the C1s signals became obvious when the pressure increased above 0.005 Torr at 298K, and it saturated after 0.0015 Torr at 298K. The C1s signal decreases when the temperature is higher than 573K. The C1s spectra indicated that the surface carbon species are consisted with two kind of components, the sp^2 and/or sp^3 carbon species at low binding energy region (282-286 eV) and CO_xH_y based species at high binding energy region (286-290 eV). Since the lower binding energy peak did not contribute to the O1s signal, we focused on the signal from the higher binding energy peak. By performing the difference spectra of both C1s and O1s at different conditions and checking the correlation between them, we can find the CO_xH_y peak located at the energy region between 530-533 eV. We considered two extreme condition: (1) the peak located at 532.2-532.5 eV, which is consisted with the observation in Kelsey's work, and (2) the peak located at 530.5-530.9 eV, which agrees with our CO_2-Ag work. Basing on these, we estimated the contribution of CO_xH_y species in the O1s spectra using 1:1 atomic ratio and added the fitting to the isothermal and isobar data as shown in the Fig.S2-S5. In Fig.S2 and S3, the contribution from carbon contamination is constrained at 532.2 eV, while in Fig. S4 and S5, the contribution form the contamination is constrained at 530.8 eV. We should notice that considering the depth profiles of C1s and O1s under 670 eV photon energy, the contribution of these species in the O1s spectra maybe overestimated, which is quite obvious in the isobar conditions. It should be specially noticed that there is no absolutely accurate method to quantify the contribution of this so-called "carbon contamination" in the O1s spectra during H_2O adsorption. Our method is a reasonable approach to address this issue. Also, after taking consideration of the contribution from the CO_xH_y species in the O1s spectra fitting under these two extreme conditions, the

good consistence between the experimental results and predicted results was not broken down.

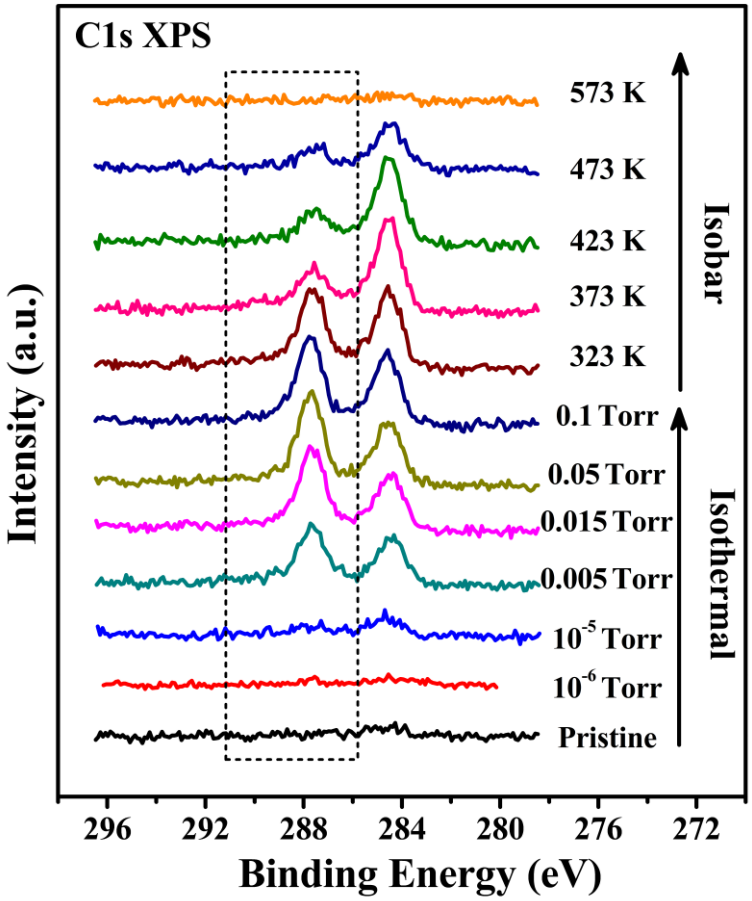

Figure S1: C1s APXPS spectra of Ag surface during H_2O adsorption under isobar and isothermal conditions.

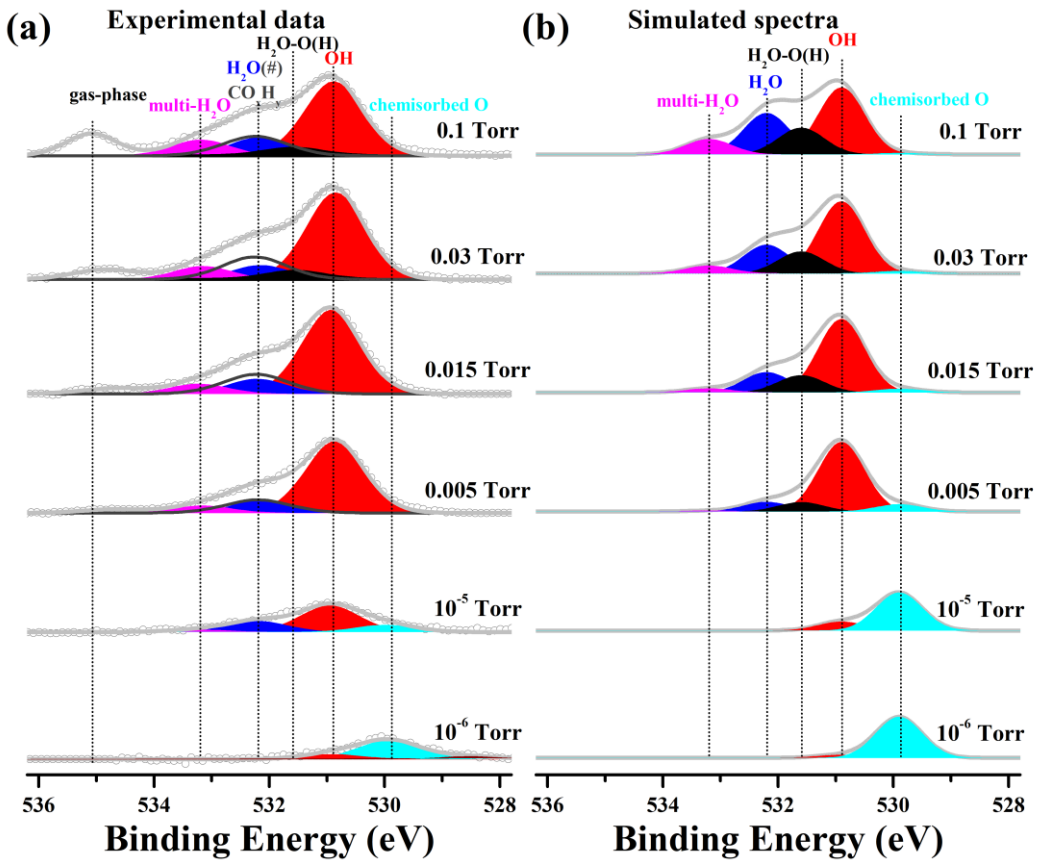

Figure S2: Comparison of experiment XPS spectrum and theory spectrum under isothermal condition at 298 K. We included the possible effect of surface CO_xH_y contamination, showing in the dark grey lines located at around 532.2 eV.

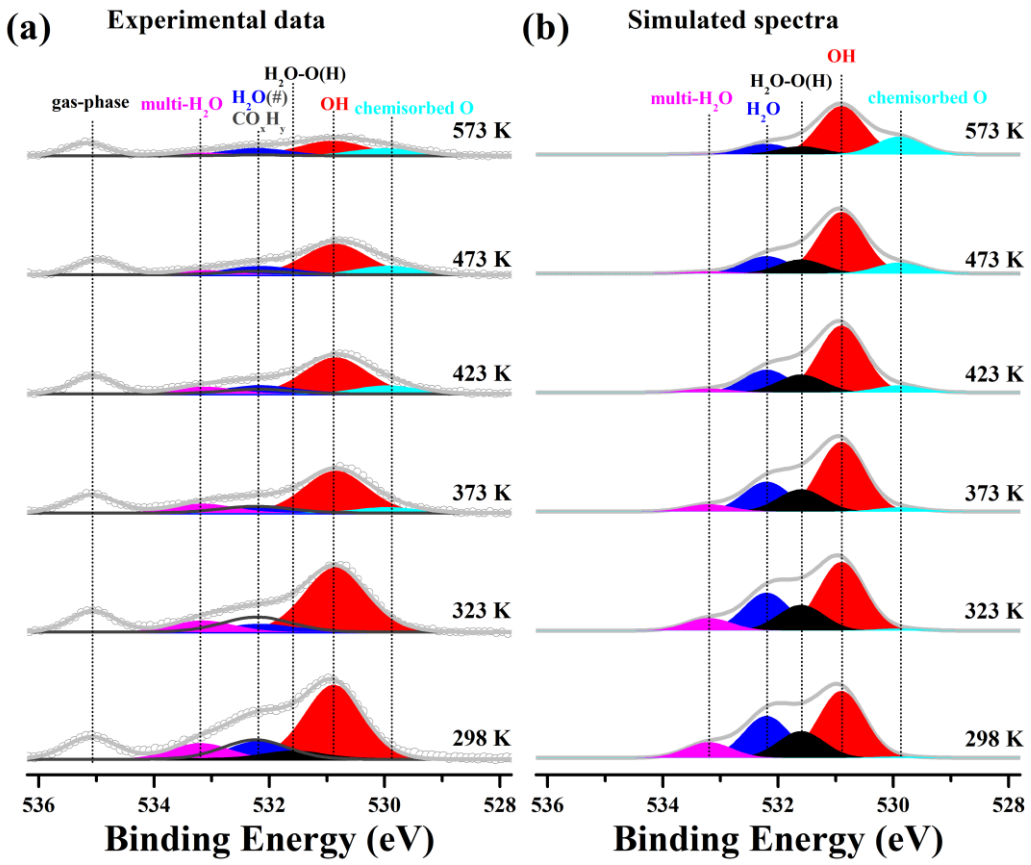

Figure S3: Comparison of experiment XPS and theory spectra under isobaric condition at 0.1 Torr. We included the possible effect of surface CO_xH_y contamination, showing in the dark grey lines located at around 532.2 eV.

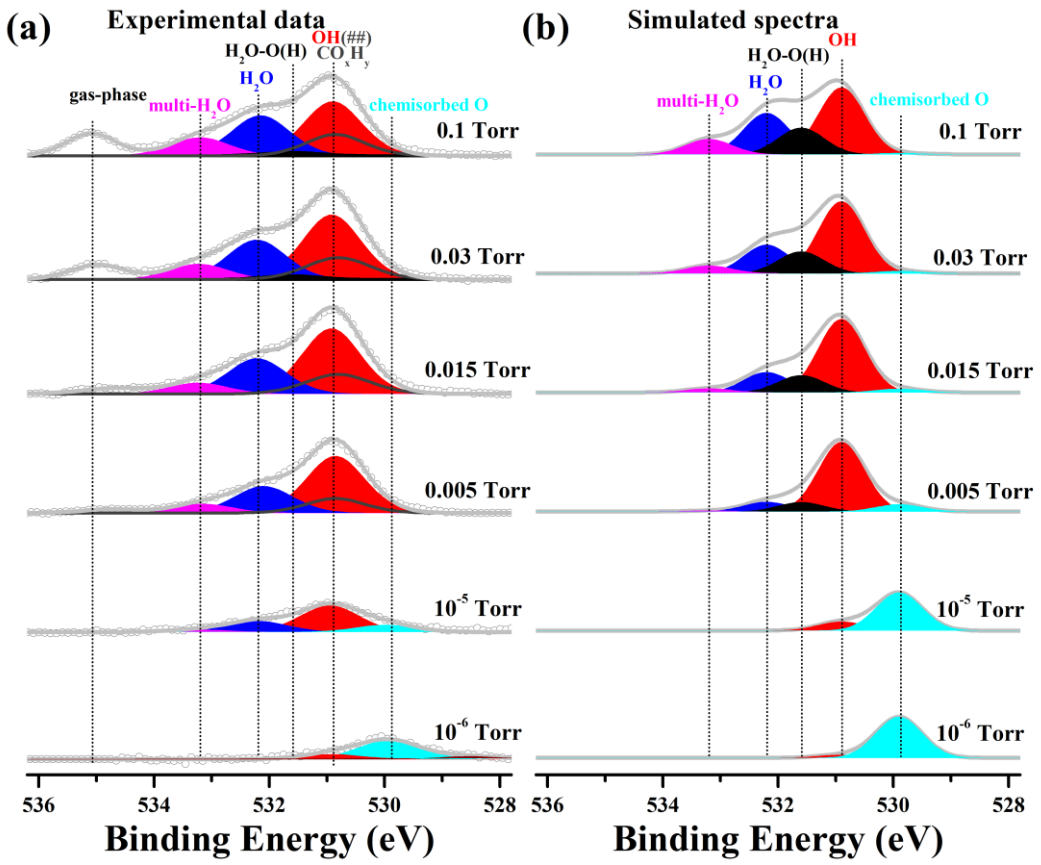

Figure S4: Comparison of experiment XPS spectrum and theory spectrum under isothermal condition at 298 K. We included the possible effect of surface CO_xH_y contamination, showing in the dark grey lines located at around 530.8 eV.

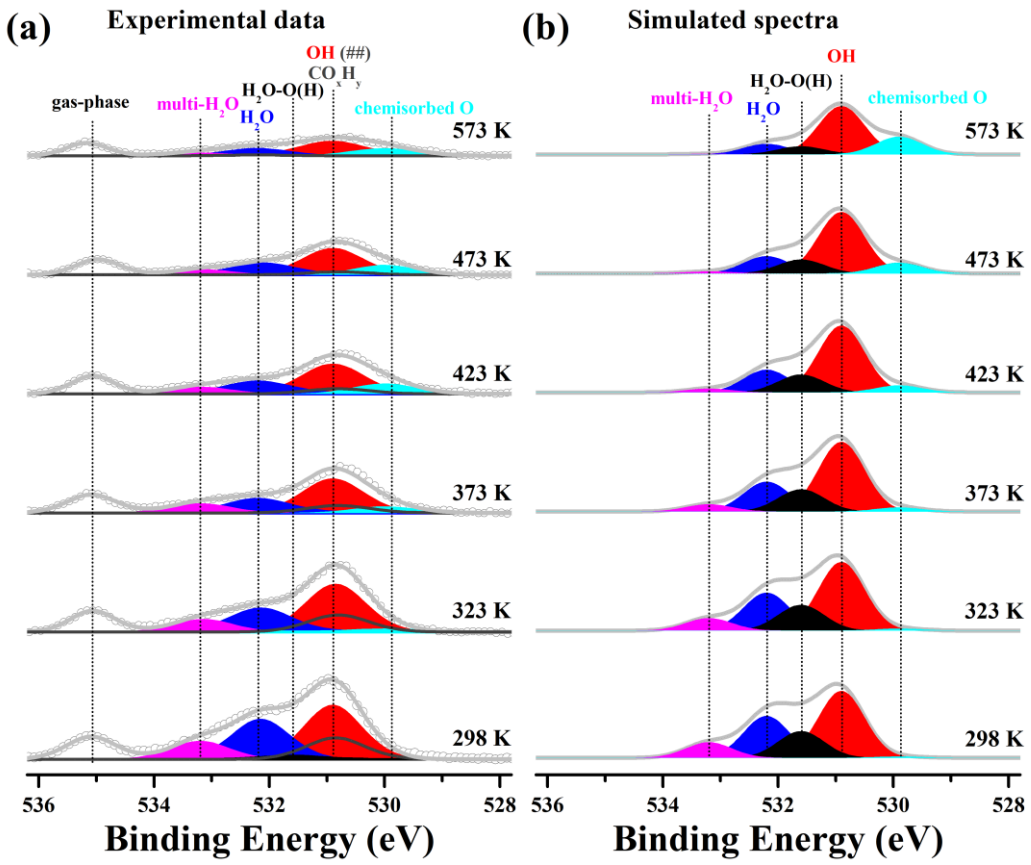

Figure S5: Comparison of experiment XPS and theory spectra under isobaric condition at 0.1 Torr. We included the possible effect of surface CO_xH_y contamination, showing in the dark grey lines located at around 530.8 eV.

		Pressure	100 mtorr	50 mtorr	30 mtorr	15 mtorr	5 mtorr	10^{-3} mtorr
		Temeratur e	298 K	298 K	298 K	298 K	298 K	298 K
	initial	final	ΔG	ΔG	ΔG	ΔG	ΔG	ΔG
adsorption	x4 + y1	x54	-0.28	-0.26	-0.24	-0.23	-0.20	0.02
adsorption	x3 + y1	x53	-0.14	-0.12	-0.11	-0.09	-0.06	0.16
reaction	x54	2*x3	-0.32	-0.32	-0.32	-0.32	-0.32	-0.32
diffusion	x53	x2+x3	0.28	0.28	0.28	0.28	0.28	0.28

diffusion	x54	x2+x4	0.41	0.41	0.41	0.41	0.41	0.41
desorption	x2	y1	-0.14	-0.16	-0.17	-0.19	-0.22	-0.43
adsorption	y1	x2	0.14	0.16	0.17	0.19	0.22	0.43
desorption	x53	x3 + y1	0.14	0.12	0.11	0.09	0.06	-0.16
desorption	x54	x4 + y1	0.28	0.26	0.24	0.23	0.20	-0.02
adsorption	x53 + y1	x6	-0.01	0.01	0.02	0.04	0.07	0.29
desorption	x6	x53 + y1	0.01	-0.01	-0.02	-0.04	-0.07	-0.29
	x3 + x3	x54	0.32	0.32	0.32	0.32	0.32	0.32

Table S1. Formation energy ΔG as a function of pressure from the QM based CRN. Example pressure conditions from 10^{-6} to 0.15 Torr are included here. For a complete table of surface species concentration with finer grids and larger scope of temperature and pressure condition, please refer to the big datasheet *result.txt*.

Discussion of core-level shift calculation and CRN kinetics

Core Level Shift Calculation

The relative XPS core-level shift of 6 identified oxygen containing species are calculated in VASP. There are two approaches for the calculation of relative core-level shift: the initial and final approximation. In the initial state approximation, Kohn-Sham eigenvalues of the core states is subsequent to the self-consistent determination of the charge density associated with the valence electrons. [2] Theoretical studies report that initial approach often reproduce the experimental observations very well [3-4], especially if the adsorbates are far from the metal surfaces, where the relaxation time is longer than near metal core-hole pair. We found that using initial state approximation generate very good agreement with experiments (within 0.2 eV difference) in this current system. However, the more sophisticated final approximation which allows the relaxation of core-hole pair is especially preferred for species such as chemisorbed oxygen, and in the current study we found that final state approximation can yield almost perfect agreement with the experimental relative core-level shift values, to be specific with the electron count of the excited electron to be 0.1 - 0.2 range.

CRN Kinetics

The core CRN solver uses Mathmatica, NDSolve. The bridging between different temperature and pressure, the analysis and visualization are customized in Python. The convergence of non-linear ODEs and the stability of numerical solution are very thoroughly discussed elsewhere. [5] We ran the simulation until steady state concentration is reached, ranging from minute time (60s) scale for low pressure (10^{-6} Torr) to hour time (5000s) scale for high pressure (1 Torr).

For the current CRN of 12 reactions, the initial concentration of O* is extrapolated from experiment to be 0.25 ML, where we used as the initial boundary condition. Each species' concentration is bound by 0 ML to 1 ML in order to give appropriate physical meaning.

Comparison of energy using D3 parameter vs. experimental lattice parameter

We have investigated two sets of lattice parameter (D3 vs. experiment [6]) to demonstrate that the energetics we used in CRN is not affected by this choice of lattice parameter (D3 vs. experiment) as long as the choice is consistent, see Table S2.

	D3_lattice	Exp_lattice	
Name	Energy(eV)	Energy(eV)	ΔE
Ag	-138.448	-138.376	0.072
Ag_x4_O	-144.081	-143.971	0.110
Ag_x3_OH	-148.877	-148.796	0.080
Ag_x2_H_2O	-153.045	-152.949	0.096
Ag_x5_2_O.H_2O	-158.792	-158.719	0.074
Ag_x5_OH.H_2O	-163.750	-163.669	0.081
Ag_x6_multi	-178.446	-178.361	0.085

Table S2 Comparison of energy using D3 parameter vs. experimental lattice parameter.

Comparison of energy using D3 parameter vs. experimental lattice parameter

It is possible to estimate the free energy from VASP as well. We consider that the Jaguar treatment as a finite molecule is more accurate. It usually compares better with experiment. But the differences are not really significant. To further clarify this consistency, the Table S3 below shows the frequency modes calculated from VASP and from Jaguar for multiple small molecules (H_2, H_2O, NH_3 to represent 1 bond, 2

bonds, and 3 bonds respectively) at the same level of DFT, comparing with experiments. [7]

	Jaguar	error(Jaguar)	VASP	error(VASP)	Exp
molecule	NH_3		NH_3		NH_3
mode (cm-1)	1076.33	-4.92%	1015.40	-10.30%	1132
mode (cm-1)	1649.91	-4.46%	1617.63	-6.33%	1727
mode (cm-1)	1651.14	-4.39%	1623.73	-5.98%	1727
mode (cm-1)	3377.21	-1.63%	3411.86	-0.62%	3433
mode (cm-1)	3513.90	-1.43%	3510.32	-1.53%	3565
mode (cm-1)	3514.26	-1.42%	3512.54	-1.47%	3565
molecule	H_2		H_2		H_2
mode (cm-1)	4369.89	-0.71%	4686.18	6.47%	4401
molecule	H_2O		H_2O		H_2O
mode (cm-1)	3702.20	-0.75%	3730.75	0.02%	3730
mode (cm-1)	1632.34	-4.60%	1591.87	-6.96%	1711
mode (cm-1)	3821.86	-0.76%	3837.30	-0.36%	3851
average		**-2.51%**		**-2.71%**	

Table S3 Consistency between Jaguar and VASP frequency modes vs. experimental data.

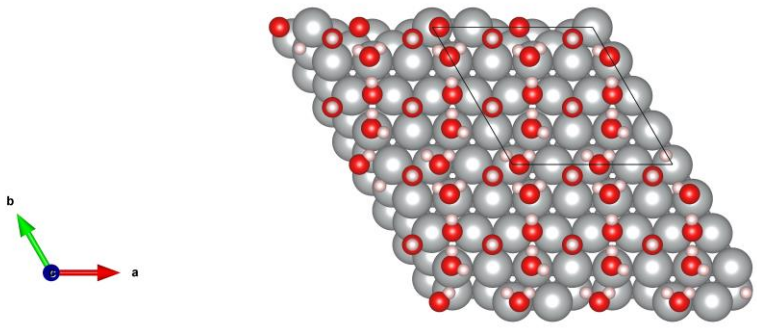

Figure S6: Hypothetical atomic illustration of high pressure (1Torr) surface species. (In contrast to the direct visualization of Figure 5 in main text.)

Reference

(1) Stoerzinger, K. A.; Hong, W. T.; Crumlin, E. J.; Bluhm, H.; Biegalski, M. D.; Shao-Horn, Y. Water Reactivity on the LaCoO3 (001) Surface: An Ambient Pressure X-Ray Photoelectron Spectroscopy Study. *J. Phys. Chem. C* **2014**, *118* (34), 19733–19741. https://doi.org/10.1021/jp502970r.

(2) Köhler, L.; Kresse, G. Density Functional Study of CO on Rh(111). Phys. Rev. B: Condens. Matter Mater. Phys. 2004, 70, 165405.

(3) Morikawa, Y.; Hayashi, T.; Liew, C. C.; Nozoye, H. First Principles Theoretical Study of Alkylthiolate Adsorption on Au (111). Surf. Sci. 2002, 507, 46−50.

(4) Taucher, T. C., Hehn, I., Hofmann, O. T., Zharnikov, M., & Zojer, E. (2016). Understanding chemical versus electrostatic shifts in X-ray photoelectron spectra of organic self-assembled monolayers. J. Phys. Chem. C 2016, 120, 6, 3428-3437.

(5) Butcher, John Charles. Numerical methods for ordinary differential equations. John Wiley & Sons, 2016.

(6) Kittel, C. *Introduction to Solid State Physics*; Wiley, 2005.

(7) ChemTube3D http://www.chemtube3d.com